Available on CMS information server

CMS CR -2015/378

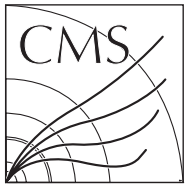

The Compact Muon Solenoid Experiment

Conference Report

Mailing address: CMS CERN, CH-1211 GENEVA 23, Switzerland

27 December 2015 (v8, 02 February 2016)

ATLAS/CMS Probing PDFs and soft QCD at the LHC

Grigory Safronov for the "Standard Model, QCD, W,Z,DIFF,FW", ATLAS and CMS collaborations.

Abstract

LHC has delivered 30 fb^{-1} of proton-proton collisions at center-of-mass energies of 7 and 8 TeV in 2010-2012 during the LHC Run I. Run II has started in 2015 and approximately 200 pb^{-1} of proton-proton collisions at $\sqrt{s} = 13$ TeV have been delivered by September. An important part of physics program in ATLAS and CMS experiments are precision studies of quantum chromodynamics (QCD). Parton density functions (PDFs) are an essential part of calculation of any process at hadron collider. Detailed studies of soft proton-proton interactions and production of soft particles allows to improve phenomenology of processes in non-perturbative QCD domain. A selection of measurements probing PDFs and soft QCD based on Run I data as well as early results from Run II are presented in this review.

Presented at *LHCP2015 The 3rd Conference on Large Hadron Collider Physics*

Probing PDFs and soft QCD at the LHC

Grigory Safronov[1,a)]

[1]*Institute for Theoretical and Experimental Physics, 117218, Moscow, B. Cheryomushkinskaya 25*

[a)]On behalf of the ATLAS and CMS Collaborations

Abstract. LHC has delivered 30 fb^{-1} of proton-proton collisions at the center-of-mass energies of 7 and 8 TeV in 2010-2012 during the LHC Run I. Run II has started in 2015 and approximately 200 pb^{-1} of proton-proton collisions at $\sqrt{s}$ = 13 TeV have been delivered by September. An important part of physics program in the ATLAS and CMS experiments are precision studies of the quantum chromodynamics. Parton density functions are an essential part of calculation of any process at a hadron collider. Detailed studies of soft proton-proton interactions and production of soft particles allows to improve phenomenology of processes in non-perturbative QCD domain. A selection of measurements probing PDFs and soft QCD based on the Run I data as well as early results from the Run II are presented in this review.

INTRODUCTION

The appropriate theory to describe interactions of hadrons is the Quantum Chromodynamics (QCD). A fundamental property of QCD is the strong dependence of the coupling constant, α_s, on the energy scale of the interaction, Q. Processes involving large Q: $Q \gg \Lambda_{QCD} \sim 200$ MeV can be described by means of the calculations based on the perturbation theory in QCD (pQCD) because the coupling constant is small, such processes are usually referred to as hard processes. Softer processes cannot be calculated perturbatively and are described by various QCD-based models with parameters fitted to the data. Monte Carlo generators widely used to simulate final states at LHC exploit such models for a simulation of a soft processes occurring in the hadron scattering such as hadronisation or multiple parton interactions.

Parton density functions (PDFs) is an essential component for calculation of any process at a hadron collider. Due to the soft nature of processes governing the state of partons inside the nucleon it cannot be calculated in the pQCD framework. It is the QCD factorization theorem which allows to factorize the total process cross-section into the hard matrix element involving interacting partons and to the probabilities to find such partons inside the proton or parton density functions which are extracted from an experiment. PDFs are parametrised as a function of the fraction of total proton momentum carried by the parton, x, and the momentum transfer in the interaction, Q. Parametrisations of PDFs are fitted to various observables using theory predictions involving leading order (LO), next-to-leading order (NLO) or next-next-to-leading order (NNLO) matrix elements.

LHC has delivered a total of approximately 30 fb^{-1} of proton-proton collisions at $\sqrt{s}$ =7 and 8 TeV during the Run I. Also data at $\sqrt{s}$ = 900 GeV and 2.76 TeV is available. The LHC Run II started in 2015 and approximately 200 pb^{-1} of proton-proton collisions at $\sqrt{s}$ = 13 TeV have been delivered by September. In this report the selection of ATLAS and CMS measurements based on the above data and sensitive to soft QCD processes and PDFs is presented.

ATLAS AND CMS DETECTORS

ATLAS and CMS are large multi-purpose detectors at the LHC collider. Tracking system of ATLAS (A Toroidal LHC ApparatuS) [1] consists of the silicon pixel, silicon micro-strip and transition radiation detectors. These detectors are surrounded by the super-conducting solenoid which provides magnetic field of 2 T. For the Run II, a new innermost layer of the silicon pixel tracker, called insertable B-layer (IBL) [2, 3], has been inserted at a radial distance of 3.3 cm from the beam line. ATLAS has Lead/Liquid Argon (LAr) sampling electromagnetic calorimeter which covers pseudorapidity (η) range $|\eta| < 3.2$. The hadron calorimeter consists of iron/scintillator barrel region ($|\eta| < 1.475$). The

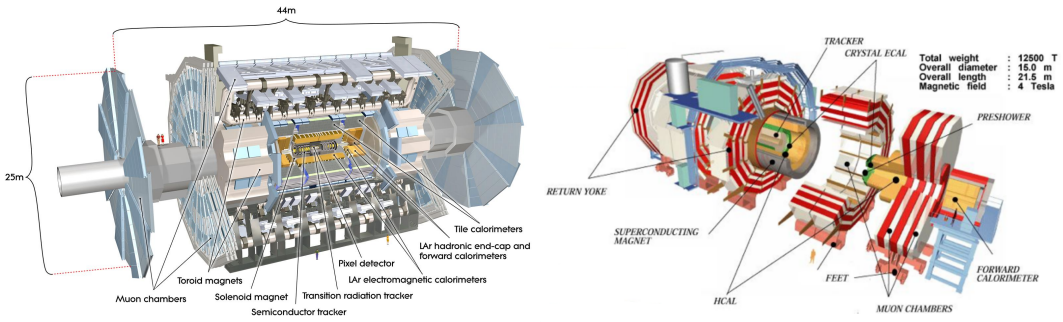

FIGURE 1. ATLAS (left) and CMS (right) detectors

endcap ($|\eta| < 3.2$) and forward ($|\eta| < 4.9$) regions are covered by *LAr* calorimeters. The ATLAS muon system is based on three large toroidal magnets with 8 coils each providing magnetic field of 2.0-7.5 T. Inside the magnets system of precision tracking chambers is located.

CMS (Compact Muon Solenoid) [4] detector is based on the super-conducting magnet providing magnetic field of 4 T. Inside the magnet the tracking system, electromagnetic and hadronic calorimeters are located. CMS tracking system consists of the pixel vertex detector and the silicon strip tracker. The electromagnetic calorimeter is made of $PbWO_4$ crystals and covers pseudorapidity range $|\eta| < 3.0$. The barrel and endcap hadronic calorimeters are sampling brass/scintillator and also cover the pseudorapidity range $|\eta| < 3.0$. The forward calorimeter covering range $|\eta| < 5.0$ is steel absorber/quartz fiber, Cerenkov light emitted in quartz fibers aligned along the beam axis is collected with photomultipliers. The magnet is surrounded by the iron return yoke with the muon drift chambers embedded into it.

SOFT QCD

Measurements of soft processes at LHC are special in a sense that they require special datasets. Data for mainstream measurements like the Higgs boson production, rare standard model processes and searches beyond the standard model is delivered with large number of pp interactions (tens) occurring in the same bunch-crossing referred to as pileup. Soft processes are extremely hard to study in the high-pileup environment because it is often not possible to distinguish objects produced in the same pp interaction. At the same time many soft measurements are not luminosity-demanding. Thus soft QCD probes are made using special low-pileup data delivered during a limited number of special low-pileup LHC fills or on other occasions.

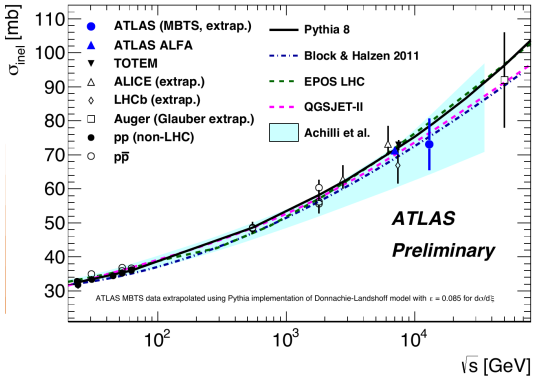

FIGURE 2. Inelastic cross-section measurement at 13 TeV by ATLAS collaboration [10]. Results from previous measurements are also shown. Data points are compared to predictions from PYTHIA8 and cosmic ray MC generators EPOS and QGSJET-II.

Cross-section of pp interactions

The milestone measurement for each energy of the LHC collisions is the pp interaction cross-section. Total cross-section cannot be calculated from the first principles but follows a number of fundamental relations one of them is the optical theorem which states that imaginary part of the forward elastic scattering amplitude is proportional to the total pp cross-section. ATLAS ALFA detector and TOTEM experiment installed in CMS cavern have precision coordinate detectors which can be moved very close to the beam ($\sim 10\sigma$ beam transverse size) and thus measure the cross-section for elastic scattering of protons differentially by Mandelstam $|t|$ variable and later extrapolate to $|t| = 0$ to make use of the optical theorem and determine the total cross-section. Measurements for 7 and 8 TeV collision energies are available from these devices based on the Run I data e.g. [5, 6, 7]. Limited in acceptance inelastic cross-section measurements are also available both from the ATLAS and CMS Collaborations from the Run I data [8, 9]. Most recent inelastic cross-section measurement was performed by the ATLAS Collaboration for 13 TeV pp collisions [10]. Inelastic scattering incorporates dissociation of at least one of the scattered protons by means of color exchange or exchange by colorless object called Pomeron, latter class of events is referred to as diffraction. Limited geometrical acceptance allows to measure cross-section in the fiducial region which is usually defined in terms of variable $\xi = M_X^2/s$, where M_X is higher mass of two observed dissociation systems. For the ATLAS measurement events were selected with the system of Minimum Bias Trigger Scintillators (MBTS) covering range of $2.07 < |\eta| < 3.86$ which provide an access to $\xi > 10^{-6}$. The fiducial cross-section was extrapolated then to the full acceptance region using different Monte-Carlo models which give a spread of ±4.7% in the final cross-section value. Final result (Fig. 2) demonstrates agreement with previous measurements although it struggles from large uncertainty of preliminary integrated luminosity measurement.

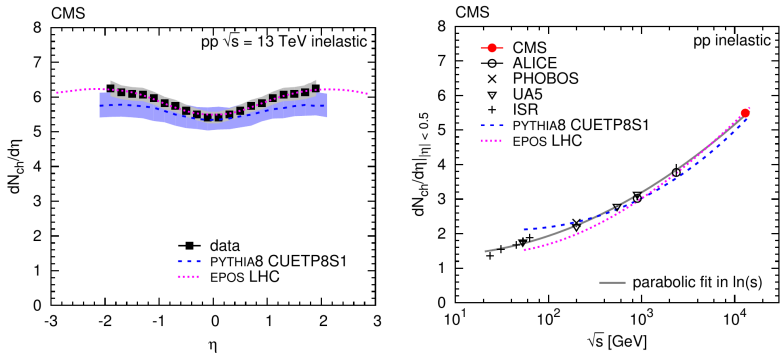

FIGURE 3. CMS results [14]. Angular distribution of charged particle density (left) in pp collisions at 13 TeV. Collision energy dependence of charged particle density in the central region (right). Measurement was performed with the 0 T magnetic field. Presented result is based on counting of straight tracks. Results were cross-checked with the method based on counting triplets of hits. Events were recorded with the Zero Bias trigger. Results are compared to the PYTHIA 8 and cosmic ray MC EPOS predictions. EPOS predictions demonstrate good agreement with the data.

Soft particle production

Angular or transverse momentum distributions of soft charged particles produced in proton-proton collisions are non-demanding measurements in terms of the number of events needed and thus can be performed at a very early stage of data-taking. Soft particle production observables allow to test models for hadronisation or multiple-parton interactions (MPI) as implemented in various Monte Carlo generators. They provide valuable input to new tunes of model parameters (along with other observables). Both ATLAS and CMS experiments have performed measurements of soft particle production in the beginning of Run I [11, 12]. Also remarkable combined measurement of soft particle production by CMS and TOTEM experiments at $\sqrt{s} = 8$ TeV is available [13] where charged particle density in pseudorapidity bins ($dN_{ch}/d\eta$) is measured up to $|\eta| = 7.0$. Recently CMS has published the paper with $dN_{ch}/d\eta$ measurement at 13 TeV (Fig. 3) [14] which is based on the data taken in special run in May 2015 with the pileup of 0.05. The preliminary results from ATLAS [15] are somewhat more extended: $dN_{ch}/d\eta$, multiplicity and transverse momentum (p_T) spectrum measurements are available, some of them are presented at Fig. 4.

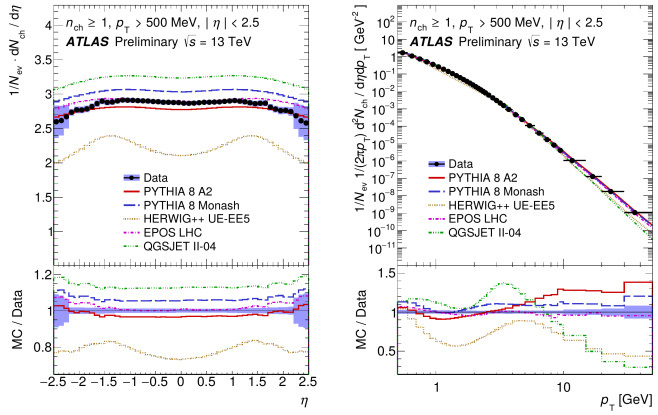

FIGURE 4. ATLAS measurement of soft particle production [15]. Charged particle density as a function of η (left) and as a function of p_T (right). Measurement was performed with 170 μb^{-1} of 13 TeV pp collisions taken in the beginning of the Run II of the LHC. Events were selected with MBTS system. Tracks with $p_T > 500$ GeV are selected for the measurement.

An interesting feature of the presented results is that EPOS MC generator [16] used for cosmic ray physics demonstrates the best agreement with the data in the wide range of pseudorapidity and p_T while well-known PYTHIA8 and HERWIG++ show some disagreements. EPOS is based on the parton-based Gribov-Regge theory and describes pp interaction in analogue to the heavy ion interaction with subsequent stages from quark-gluon plasma to freeze-out. The key observable for fit to data is the total cross-section and the inelastic cross-section. Although fits to other soft observables are also used [16].

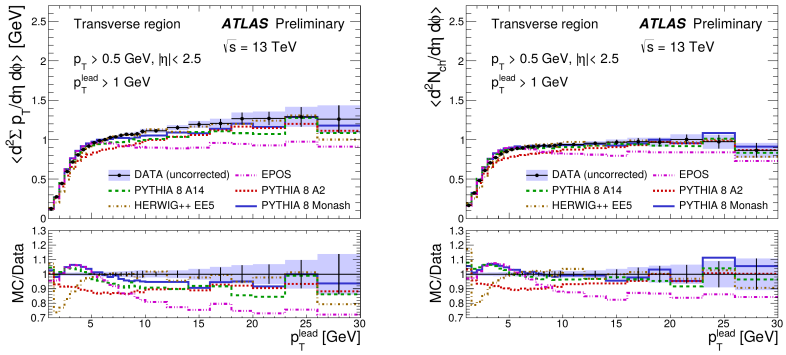

FIGURE 5. ATLAS underlying event measurement [21]. The density of scalar p_T sum (left) and the multiplicity density (right) in the transverse region as a function of the leading track transverse momentum, p_T^{lead}. Sample of 170 μb^{-1} was used for the measurement. The data points are not corrected for the detector effects. The data is compared to MC predictions passed through the full ATLAS detector simulation.

The key measurement for understanding soft activity in the presence of a hard probe and thus for tuning of the Monte-Carlo generators which incorporate hard physics like PYTHIA8 or HERWIG++ is the underlying event (UE) measurement. The underlying event activity consists of particles emerging from hadronisation of soft initial- and final- state radiation, products of MPI and beam remnants. Understanding of UE is important for many new physics searches and precision studies of the standard model. In particular UE contaminates isolation variables and creates an offset to the jet energy measurement. An event topology in transverse to the beam plane is divided to "toward" and "away" regions defined by the leading jet (or particle) direction and "transverse" region in which the underlying event properties are measured. Normally the number of particles and average p_T per unit of solid angle are measured as a function of the transverse momentum of the leading jet (or particle), p_T^{lead}. The underlying event was first defined and measured by the CDF collaboration in $p\bar{p}$ collisions at $\sqrt{s} = 1.8$ TeV [17] and since then has been widely used for

tuning of general-purpose MC generators. ATLAS and CMS provided UE measurements based on the 0.9, 2.76 and 7 TeV data [18, 19, 20] which were used for Run I -based MC tunes. Recently the measurement from ATLAS based on 13 TeV data [21] has become available. Results of the measurement are presented at Fig. 5, they are not corrected for the detector effect and thus compared to the Monte Carlo predictions passed through the full detector simulation. The PYTHIA 8 tunes A2, A14 and Monash were used for comparison. The former two tunes were developed by the ATLAS collaboration and are aimed at the description of a soft particle production observables (A2) or an underlying event- and parton shower- sensitive observables (A14). Monash tune was developed by the PYTHIA 8 authors and is optimized for the description of energy dependence of soft particle production and underlying event data. HERWIG++ tune UEE5 is optimized for the good description of the underlying event at 7 TeV. Data points are well-described by the PYTHIA 8 and HERWIG++ tunes except for the region of the plateau onset: $1 < p_T^{lead} < 5$ GeV. The EPOS MC fails as the hardness of the probe object increases.

Two-particle correlations

A study of particle correlations provide further insight into the nature of soft QCD processes in particular about collective effects during the collision of protons. Angular two-particle correlations studied as 2-dimensional correlation function in $\Delta\eta - \Delta\phi$ coordinates are discussed in this paragraph. The strong particle correlation referred to as "long-range far-side" correlation is demonstrated for $\Delta\phi \sim \pi$ due to the momentum conservation law. It was the remarkable result of the LHC Run I when CMS has observed the correlation of particles produced with similar ϕ (or $\Delta\phi \sim 0$) along the η coordinate in proton-proton collisions with large particle multiplicity [22]. Such correlation referred to as "long-range near-side" has been observed earlier in heavy ion collisions e.g. by PHOBOS collaboration [23]. The observation has received wide attention from theory community and a broad range of models was suggested to explain the correlation [24]. Preliminary ATLAS Collaboration results on the two-particle correlations in pp collisions at 13 TeV are available in [25] and by the time of the writing the updated results have become available in [26], Fig. 6. The measurement was performed with 14 nb^{-1} of the low-pileup pp collisions. Dedicated trigger which required at least 60 tracks with $p_T > 0.4$ GeV was used to select the events. The two-particle correlation was measured in bins of the charged particle multiplicity, N_{ch}^{rec}. Which is defined as the number of tracks with $p_T > 0.4$ GeV originating from the vertex with the largest Σp_T^2 in the event. The correlation function is defined as $C(\Delta\phi, \Delta\eta) = S(\Delta\phi, \Delta\eta)/B(\Delta\phi, \Delta\eta)$ where S and B correspond to charged particle pairs taken from the same event and from mixed events respectively. In addition the yield of particles per selected particle, Y, was measured. The yield quantifies strength of the correlation and represents the number of particles associated with each trigger particle in a given $\Delta\phi/\Delta\eta$ interval. An excess of the yield over uncorrelated background integrated over the "ridge" area, Y_{int} (Fig. 6), is consistent with zero for $N_{ch}^{rec} < 40$ and increases rapidly with N_{ch}^{rec} for $N_{ch}^{rec} > 40$. ATLAS measurement of Y_{int} is consistent with the CMS 7 TeV result. This suggests a statement that the strength of the correlation in the "ridge" does not depend on the collision energy.

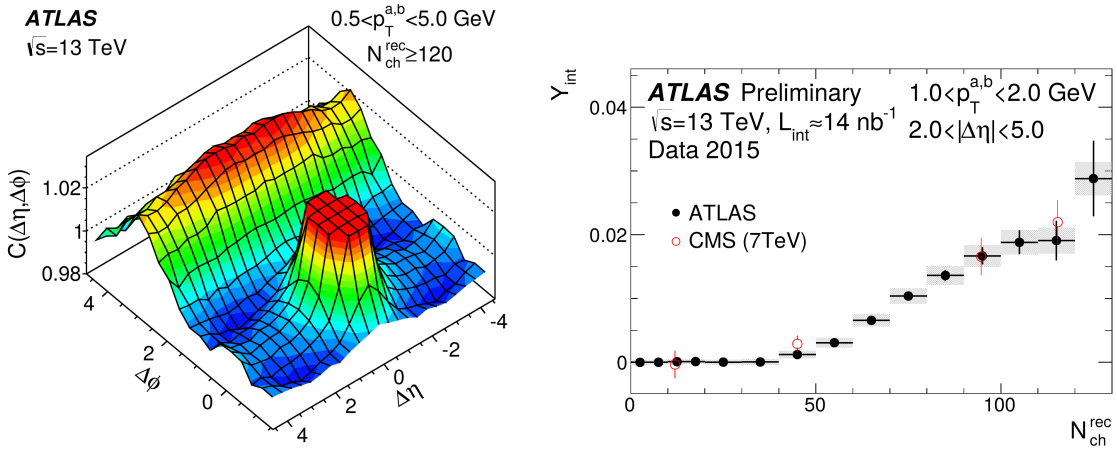

FIGURE 6. Measurement of the two-particle correlations from ATLAS. The two-dimensional correlation function, $C(\Delta\phi, \Delta\eta)$ from [26] (left). The integrated yield of particles within the ridge per selected particle with subtracted uncorrelated background from [25] (right) . An agreement with the 7 TeV CMS data is demonstrated.

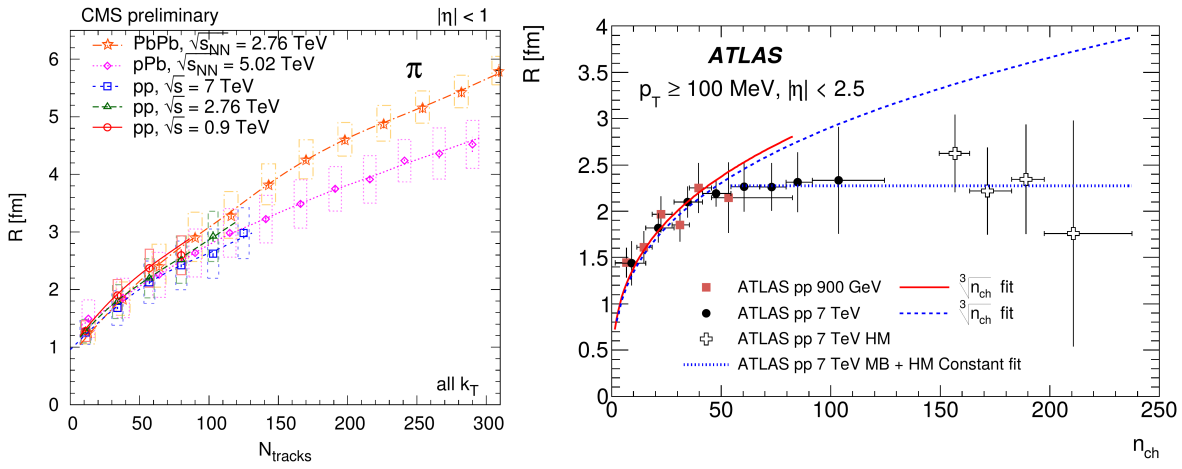

FIGURE 7. Measurements of the Bose-Einstein correlations. The CMS results from [30] (left) show that interaction region size, R, as a function of the multiplicity of charged tracks (N_{tracks}) is the same for heavy ion and pp collisions and for different energies. In the ATLAS results from [29] (right) the saturation of R is observed for pp collisions and the charged particle multiplicity, n_{ch}, greater than 55.

Due to the fact that wave function of 2-boson system is symmetric under the interchange of particles the probability to observe two identical bosons is increased. This statement makes basis for the long-standing "Bose-Einstein correlation " (BEC) method for the determination of size of a boson-emitting source used in the astrophysics and particle physics. CMS has measured BEC in 900 GeV, 2.76 and 7 TeV data [27, 28]. ATLAS has measurements at 900 GeV and 7 TeV [29]. Bose-Einstein correlations are measured in terms of the correlation function: $C = \rho(p_1, p_2)/\rho_0(p_1, p_2)$, where ρ is the spatial density of particles close in momentum space while ρ_0 is the same density for the so-called reference sample which should include all types of particle correlations except for the BEC. Different methods for constructing the reference sample are being used. CMS in [27] has used particles harvested from different events while ATLAS in [29] used opposite-sign pairs. Both collaborations use the ratio of the correlation function to the analogous function obtained from MC simulation which does not include BEC effects to correct for detector effects and resonance decays. Both collaborations study BEC as a function of charged particle multiplicity. CMS both in [28] and [27] has proved that the interaction region size, R, does not depend on the collision energy. In [30] CMS compared BEC results for the pp, pPb and $PbPb$ collisions [30] and found that the size of interaction region does not depend on whether nucleons or nuclei collide (Fig. 7 left). ATLAS in [29] has extended the measurement for pp collisions to larger multiplicities and observed the saturation of interaction region size for charged particle multiplicity greater than 55 (Fig. 7 right).

PDF PROBES

The parton density functions are of vital importance for theory predictions for any LHC measurement. Pre-LHC PDF sets are mostly constrained by the data from the HERA and Tevatron colliders. For proton-proton collisions at high values of x quark PDF dominates over gluon while at low x gluon PDF dominates. PDF uncertainties are large at very high x which is a constraining factor for new physics searches with heavy-mass states. For medium x PDF uncertainty is smaller but still gives a sizable contribution to precision studies of standard model parameters. PDF in low-x region are dominated by gluons and have large uncertainty while this region could be used for pQCD resummation studies such as applicability of DGLAP and BFKL approaches to PDF evolution description. Many PDF-sensitive measurements are available from the LHC Run I. Many of them have been incorporated into new PDF sets [31]. Recent new PDF sets CT14 [32], NNPDF3.0 [33] and MMHT14 [34] include ATLAS, CMS and LHCb data into global fits. Review of the selection of PDF-sensitive measurements from ATLAS and CMS is given below.

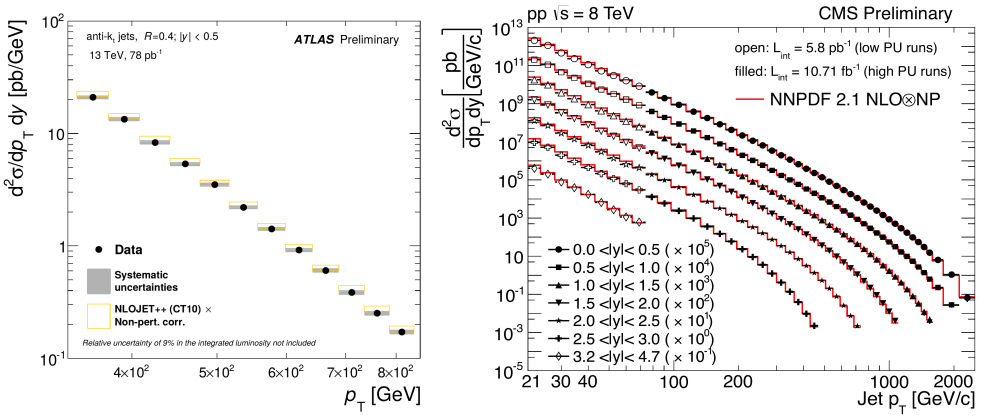

FIGURE 8. Inclusive jet measurements at 13 TeV from ATLAS [39] (left) and at 8 TeV from the CMS [37, 38] (right)

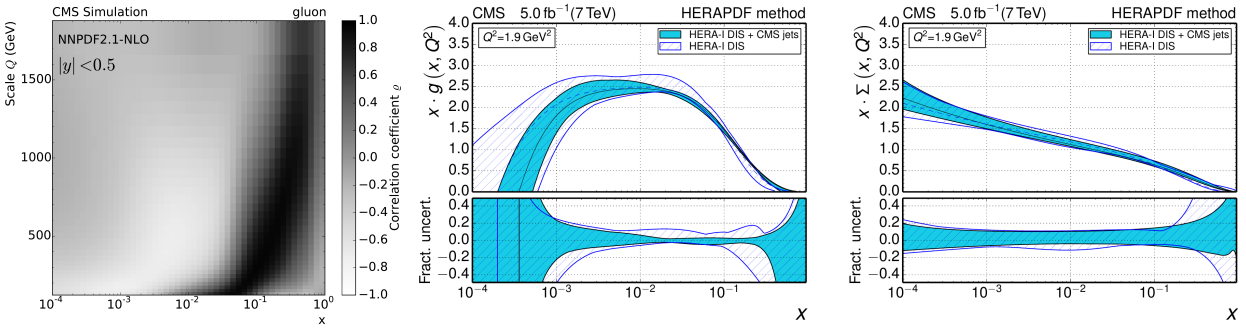

FIGURE 9. Results of PDF fit performed by CMS collaboration with 7 TeV inclusive jet data combined with HERA DIS data [40]. PDFs evolved to Q^2=1.9 GeV are shown. Significant reduction of gluon pdf (left) and quark (pdf) uncertainty is observed

Inclusive jet cross-sections

The inclusive jet cross-section provides an access to a wide range of x. Lower x jet production is dominated by gluons while for the large x jet production is dominated by quark jets. Many Run I data - based jet measurements are available from ATLAS and CMS. Both ATLAS and CMS have measured inclusive jet cross-section up to $p_T \sim 2$ TeV using the full 7 TeV collision energy dataset [35, 36]. Combination of 8 TeV CMS results for low p_T jets measured with low-pileup data [37] and high-p_T jets [38] is available (Fig. 8 right). ATLAS Collaboration has preliminary 13 TeV result [39] (Fig. 8 left). Results are compared to NLO calculation corrected for non-perturbative effects, good agreement of theory predictions with the data is observed.

Both Collaborations have used an inclusive jet data for their own extractions of the PDFs and strong coupling constant [40, 41]. Such studies although not being part of any PDF set give important information on the PDF sensitivity of chosen observables. At Fig. 9 (left) the correlation between the inclusive jet cross-section and the value of gluon PDF is shown, as obtained by CMS in [40]. Gluon PDF is strongly correlated with the cross-section except for the largest x where the jet cross-section is determined by quarks. CMS has performed PDF extraction from combined CMS 7 TeV and HERA DIS data. Results are presented at Fig. 9 (center and right). Gluon PDF uncertainty is reduced in the wide range of x, while for quark PDF uncertainty improvement is demonstrated for large x.

ATLAS has used the inclusive jet cross-section measurement [36] in combination with the jet cross-section measured in 0.2 pb^{-1} of 2.76 TeV collisions for the PDF extraction [41]. Fig. 10 shows the ratio of cross-sections at 7 TeV and at 2.76 TeV, ρ, divided by theory predictions obtained with CT10 PDF set. Systematic uncertainty on the ratio is very small which is the result of partial cancellation of correlated detector-related uncertainties. Thus combined data might bring new constraint on the PDF. At Fig. 11 results of the combined fit for HERA DIS data and the ATLAS jet

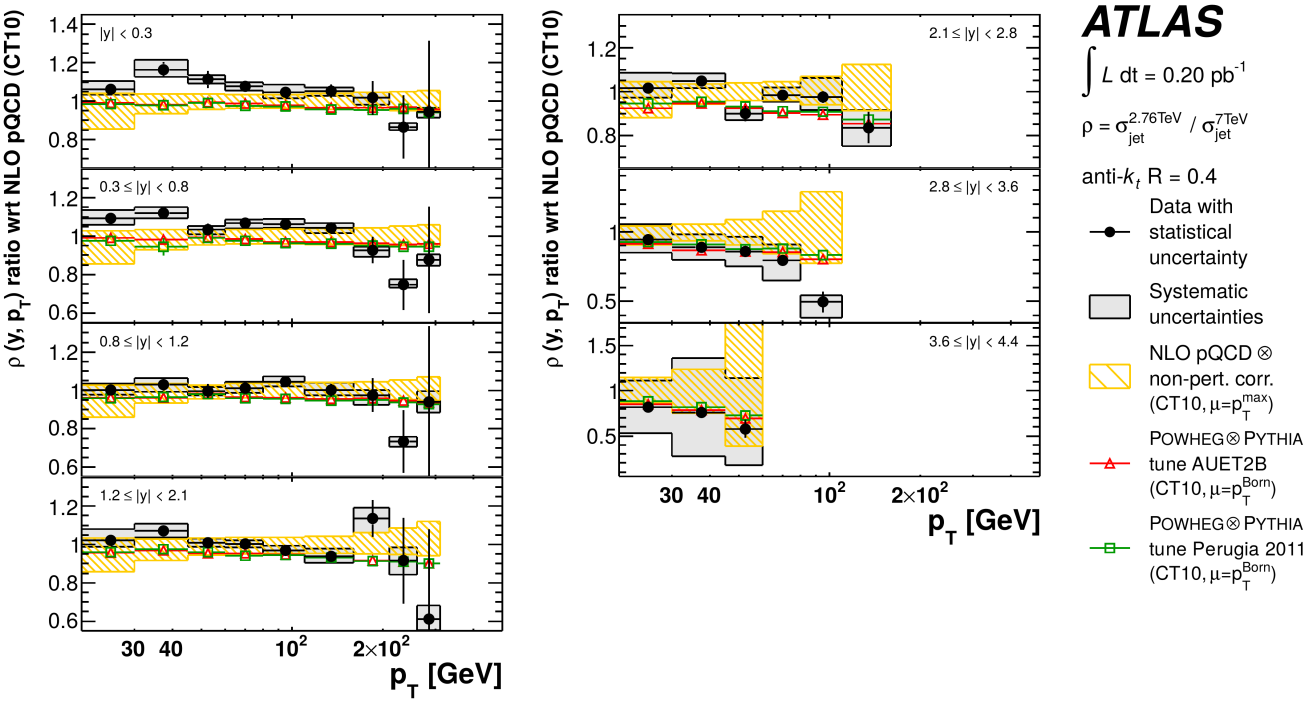

FIGURE 10. ATLAS measurement of the ratio of inclusive jet cross-section at different energies [41]. Ratio of the inclusive jet cross section at $\sqrt{s} = 2.76$ TeV to cross-section at $\sqrt{s} = 7$ TeV divided by the ratio obtained in NLO calculation with CT10 PDF set shown as a function of the jet p_T in bins of the jet rapidity y. The 4.3% uncertainty from the luminosity measurement is not shown.

data for gluon PDF is shown. Combined fit brings shift to central value and improvement in PDF uncertainty.

CMS has measured the inclusive jet cross-section at 2.76 TeV for 2013 dataset of 5 pb^{-1} and obtained the ratio to 8 TeV inclusive cross-section measured using 8 TeV dataset (10.71 fb^{-1}) [38].

Finally both ATLAS [42, 43] and CMS [44] have measured the double jet and tri-jet cross-sections which also can be used for the extraction of PDFs.

W, Z production

The W and Z boson production cross-sections and rapidity distributions are used for the PDF constraints since Tevatron. The ATLAS and CMS have measured W, Z cross-sections with the 13 TeV data [45, 46]. ATLAS measurements in [45] were done with 85 pb^{-1}. The total W and Z cross sections in electron and muon channels were measured as well as the ratios of cross-sections W^+/W^- and $W^\pm/Z$. The W^+/W^- ratio probes difference between valence u and d quark distributions while $W^\pm/Z$ ratio is sensitive to the strange quark content. The ratios benefit from experimental uncertainty cancellation. In general NNLO theoretical predictions with various PDF sets showed an agreement with the data except for the case of CT10 NNLO PDF set which showed moderate discrepancy for W^+/W^- ratio.

An interesting channel which allows to directly probe strange quark content inside the proton is the W + charm quark production. Production of W from u-quark is Cabibbo-suppressed and contributes few % to the total cross-section. Measurement of the $W + c/W + \bar{c}$ cross-section ratio can provide info on $s/\bar{s}$ content asymmetry. CMS has measured the cross-section and the cross-section ratio using 5 fb^{-1} of 7 TeV data [47] both integrated and differential in pseudorapidity of the lepton from W decay. Differential measurement provides an access to PDF for different values of x. W's were reconstructed in e or μ decay channel.

Similar results from ATLAS for the 4.7 fb^{-1} of 7 TeV data are available [48]. In the work [49] ATLAS has performed fit of the differential distributions with HERAPDF set with free parameter reflecting s/d quark content ratio. ATLAS data suggests that content of s and d quarks is symmetric for wide range of x (Fig. 12 left). CMS has

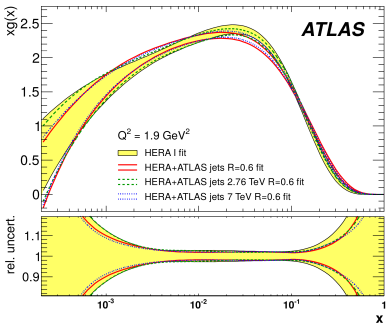

FIGURE 11. Results of combined PDF fit of to ATLAS 2.76 and 7 TeV data and to HERA DIS data [41]

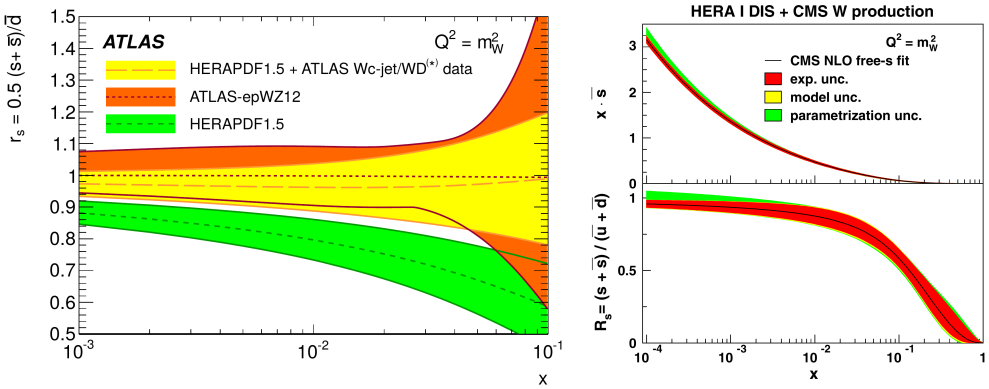

FIGURE 12. Results for the strange quark / light quark PDF extraction. ATLAS fit of $W + c$ data [48] (left), no strange quark suppression with respect to light quarks is observed. CMS fit of muon asymmetry data [50] (right), s-quark PDF is suppressed with respect to light quark PDF for medium and large x.

performed fit of ratio of s quark content to those of u and d quarks in the work [50] using both the W muon charge asymmetry and the W+charm measurements. While the QCD analysis performed by ATLAS collaboration suggests a symmetric composition in the light-quark sea at the low x region, the fit result using the CMS measurements suggests that the strange sea quark distribution is suppressed in the medium to high x region, consisting with the prediction from global PDFs (Fig. 12 right).

Drell-Yan

Along with the DIS Drell-Yan (DY) process have been used since long time for PDF extraction in dedicated fixed-target experiments. DY process is production of lepton pair in hadronic interactions via s-channel γ^*/Z boson production. Differential distributions in mass or rapidity of the produced lepton pair can be calculated up to NNLO in the perturbation theory. Rapidity and mass of the lepton pair give an access to Q and x of the interaction. Measurements of these distributions allow to probe PDFs in particular for large x. At the same time LHC energy provides an access to large values of Q never probed before. DY production has been investigated in detail both by ATLAS [51, 52] and CMS [53, 54] collaborations. Recent CMS measurement is made on the sample of 8 TeV collisions as large as 20 fb^{-1} [54]. Differential distributions of both electron and muon pairs are obtained for the mass range $m_{ll} > 15$ GeV. Differential distributions and total cross-section in the Z-peak region are compared to pQCD NNLO calculations with CT10 NNLO PDFs set. Total cross-section for the Z-peak are calculated for $60 < m_{ll} < 120$ GeV region and are found to be consistent between electron and muon channels and NNLO calculations. In the same work along with absolute cross-section CMS has measured the ratio of normalized 8 and 7 TeV cross-sections. In paper [52] ATLAS collaboration has measured differential cross-section in bins of DY mass for the very low mass range. In addition to the measurement itself the fit of PDF to measured observables using NLO and NNLO pQCD calculations was performed

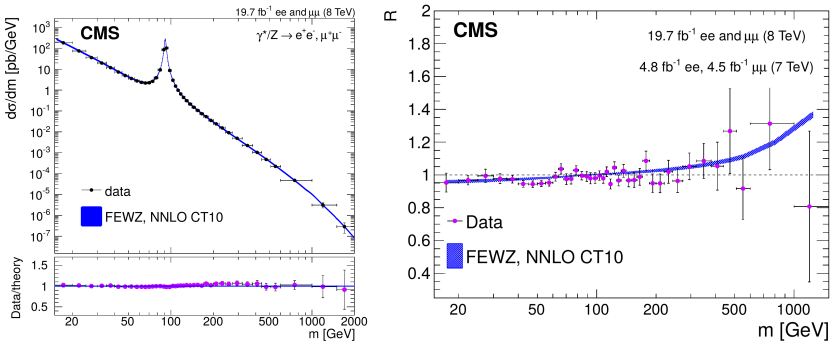

FIGURE 13. CMS results on the Drell-Yan production [54]. Cross-section (left) and the ratio of 7 and 8 TeV normalized cross-sections (right) differential in lepton pair mass.

in the ATLAS work.

CONCLUSIONS

The selection of the soft QCD measurements from the ATLAS and CMS collaborations has been discussed. Results for a many basic measurements are available for the 13 TeV pp collisions. Monte-Carlo generators tuned using Run I data show good performance with respect to the 13 TeV data. New results for two-particle correlations were discussed. The "ridge" observation in pp-collisions made by the CMS at $\sqrt{s} = 7$ TeV was for the first time confirmed by the ATLAS experiment in pp collisions at 13 TeV. An independence of strength of correlation in the ridge region on collisions energy was demonstrated. At the same time earlier CMS measurements of Bose-Einstein correlations for lower $\sqrt{s}$ showed that the size of the interaction region in pp collisions does not depend on collision energy. Recent Bose-Einstein correlation measurement from ATLAS reveals new interesting feature of collective effects in pp collisions - the saturation of interaction region size for the large multiplicities of final state charged particles.

Along with the Higgs-boson discovery Run I of the LHC has delivered many precision results which sharpen methods for theoretical calculations within the framework of the standard model. In particular the LHC data has significant impact on the global PDF fits. A number of new PDF sets which incorporate LHC Run I data have been produced and are being used for Run II analyses. New measurements with pp collisions at 13 TeV sensitive to PDF start to appear.

ACKNOWLEDGEMENTS

Author of these proceedings is supported by RFBR (Russia) grant number 14-02-31388.

REFERENCES

[1] ATLAS Collaboration, JINST **3**, S08003 (2008)
[2] M. Capeans, *et al.* (ATLAS IBL Collaboration), CERN-LHCC-2010-013, ATLAS-TDR-19
[3] ATLAS Collaboration CERN-LHCC-2012-009, ATLAS-TDR-19-ADD-1
[4] CMS Collaboration, JINST **3**, S08004 (2008)
[5] G. Antchev, *et al.* (TOTEM Collaboration), Europhys. Lett. **101**, 21002 (2013)
[6] G. Antchev, *et al.* (TOTEM Collaboration), Nucl. Phys. B **899**, 527 (2015), *arXiv:1503.08111 [hep-ex]*
[7] ATLAS Collaboration, Nucl. Phys. B **889**, 486 (2014) *arXiv:1408.5778 [hep-ex]*
[8] ATLAS Collaboration, Nature Commun. **2**, 463 (2011), *arXiv:1104.0326 [hep-ex]*
[9] CMS Collaboration, Phys. Lett. B **722**, 5 (2013), *arXiv:1210.6718 [hep-ex]*
[10] ATLAS collaboration, ATLAS-CONF-2015-038
[11] ATLAS Collaboration, New J. Phys. **13**, 053033 (2011), *arXiv:1012.5104 [hep-ex]*
[12] CMS Collaboration, Phys. Rev. Lett. **105**, 022002 (2010), *arXiv:1005.3299 [hep-ex]*

[13] CMS and TOTEM Collaborations, Eur. Phys. J. C **74**, no. 10, 2053 (2014), *arXiv:1405.0722 [hep-ex]*
[14] CMS Collaboration, Phys. Lett. B **751**, 143 (2015), *arXiv:1507.05915 [hep-ex]*
[15] ATLAS collaboration, ATLAS-CONF-2015-028
[16] T. Pierog, *et al.* Phys. Rev. C **92**, no. 3, 034906 (2015), *arXiv:1306.0121 [hep-ph]*
[17] T. Affolder *et al.* (CDF Collaboration), Phys. Rev. D **65**, 092002 (2002)
[18] ATLAS Collaboration, Phys. Rev. D **83**, 112001 (2011), *arXiv:1012.0791 [hep-ex]*
[19] CMS Collaboration, JHEP **1304**, 072 (2013), *arXiv:1302.2394 [hep-ex]*
[20] CMS Collaboration, JHEP **1109**, 109 (2011), *arXiv:1107.0330 [hep-ex]*
[21] ATLAS Collaboration, ATL-PHYS-PUB-2015-019
[22] CMS Collaboration, JHEP **1009**, 091 (2010)
[23] B. Alver, *et al.* (PHOBOS Collaboration), Phys. Rev. C **81**, 024904 (2010), *arXiv:0812.1172 [nucl-ex]*
[24] W. Li, Mod. Phys. Lett. A **27**, 1230018 (2012), *arXiv:1206.0148 [nucl-ex]*
[25] ATLAS collaboration, ATLAS-CONF-2015-027
[26] ATLAS Collaboration, CERN-PH-EP-2015-251, *arXiv:1509.04776 [hep-ex]*
[27] CMS Collaboration, CMS-PAS-FSQ-13-002
[28] CMS Collaboration, Phys. Rev. Lett. **105**, 032001 (2010), *arXiv:1005.3294 [hep-ex]*
[29] ATLAS Collaboration, Eur. Phys. J. C **75**, no. 10, 466 (2015), *arXiv:1502.07947 [hep-ex]*
[30] CMS Collaboration, CMS-PAS-HIN-14-013
[31] J. Rojo, *et al.*, J. Phys. G **42**, 103103 (2015), *arXiv:1507.00556 [hep-ph]*
[32] S. Dulat, *et al.*, *arXiv:1506.07443 [hep-ph]*
[33] R. D. Ball, *et al.*, JHEP **1504**, 040 (2015), *arXiv:1410.8849 [hep-ph]*
[34] L. A. Harland-Lang, *et al.*, Eur. Phys. J. C **75**, no. 5, 204 (2015), *arXiv:1412.3989 [hep-ph]*
[35] CMS Collaboration, Phys. Rev. D **87**, no. 11, 112002 (2013), *arXiv:1212.6660 [hep-ex]*
[36] ATLAS Collaboration, JHEP **1502**, 153 (2015), *arXiv:1410.8857 [hep-ex]*
[37] CMS Collaboration, CMS-PAS-FSQ-12-031
[38] CMS Collaboration, CMS-PAS-SMP-12-012
[39] ATLAS collaboration, ATLAS-CONF-2015-034
[40] CMS Collaboration, Eur. Phys. J. C **75**, no. 6, 288 (2015), *arXiv:1410.6765 [hep-ex]*
[41] ATLAS Collaboration, Eur. Phys. J. C **73**, no. 8, 2509 (2013), *arXiv:1304.4739 [hep-ex]*
[42] ATLAS Collaboration, Eur. Phys. J. C **75**, no. 5, 228 (2015), *arXiv:1411.1855 [hep-ex]*
[43] ATLAS Collaboration, JHEP **1405**, 059 (2014), *arXiv:1312.3524 [hep-ex]*
[44] CMS Collaboration, Eur. Phys. J. C **75**, no. 5, 186 (2015), *arXiv:1412.1633 [hep-ex]*
[45] ATLAS collaboration, ATLAS-CONF-2015-039
[46] CMS Collaboration, CMS-PAS-SMP-15-004
[47] CMS Collaboration, JHEP **1402**, 013 (2014), *arXiv:1310.1138 [hep-ex]*
[48] ATLAS Collaboration, JHEP **1405**, 068 (2014), *arXiv:1402.6263 [hep-ex]*
[49] ATLAS Collaboration, Phys. Rev. Lett. **109**, 012001 (2012), *arXiv:1203.4051 [hep-ex]*
[50] CMS Collaboration, Phys. Rev. D **90**, no. 3, 032004 (2014), *arXiv:1312.6283 [hep-ex]*
[51] ATLAS Collaboration, Phys. Lett. B **725**, 223 (2013), *arXiv:1305.4192 [hep-ex]*
[52] ATLAS Collaboration, JHEP **1406**, 112 (2014), *arXiv:1404.1212 [hep-ex]*
[53] CMS Collaboration, JHEP **1312**, 030 (2013) *arXiv:1310.7291 [hep-ex]*
[54] CMS Collaboration, Eur. Phys. J. C **75**, no. 4, 147 (2015), *arXiv:1412.1115 [hep-ex]*